FABRICATION OF A PROTOTYPE MICRO ACCELERATOR PLATFORM

Jianyun Zhou*, Joshua McNeur, and Gil Travish

Department of Physics & Astronomy, UCLA, Los Angeles, CA 90095 USA

Rodney Yoder, Manhattanville College, Purchase, NY 10577 USA

Abstract

The Micro-Accelerator Platform is a laser powered particle acceleration device made from dielectric materials. Its main building blocks, distributed Bragg reflectors and nanoscale coupling slots, are fabricated using cutting-edge nanofabrication techniques. In this report, a prototype device will be presented, and technical details of its fabrication will be discussed. Optical properties of the DBR films are measured by ellipsometry, and film surface roughness is measured using a profilometer. In addition, a few remaining challenges with the manufacture of this device will be discussed.

INTRODUCTION

The micro accelerator platform (MAP) is a laser powered, slab-symmetric dielectric structure that is only a few millimeters in size, and has been described elsewhere [1-3]. When laser pulses are driven onto the surface of the structure, the laser power is coupled into the vacuum gap between the dielectrics, forming an accelerating field which can be as high as 1GV/m. Extensive simulation work carried out at UCLA has provided a design and material selection for a prototype structure [4-5]. Fig. 1 shows an optimized structure, derived from simulations, which consists of two slab structures and a vacuum gap in between. The top slab includes a top layer with nano-sized coupling slots, matching layers, and a dielectric Bragg reflector. The bottom slab has a Bragg reflector and matching layers on a substrate. The vacuum gap in between forms the electron beam path.
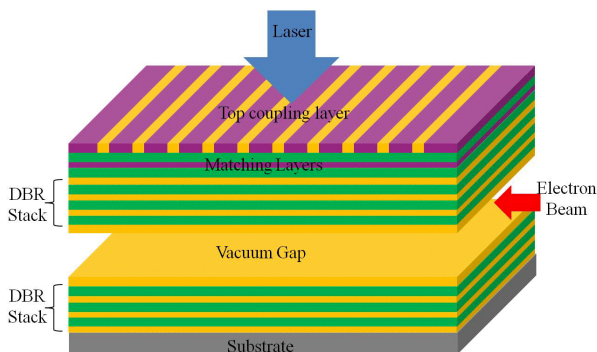

Figure 1: Illustration of the micro accelerator platform structure, consisting of coupling slots, Bragg reflectors and matching layers.

During operation, the whole structure is exposed to high power laser pulses. Therefore, all the materials used to build this platform have to be able to withstand high peak fields, in addition to having excellent optical, mechanical

and thermal properties. In the past year, after literature review and experimental testing, we have chosen ZrO_2, HfO_2 and SiO_2 to build our prototype device[2]. Here we will present the fabricated structure components, a full structure, and some optical measurement results for them. Fabrication techniques, problems and solutions associated with them will be discussed. In addition, two techniques to integrate the top and the bottom slabs for bench tests will be compared and discussed, and other challenges to the manufacture of the structure and bench test of the device will be presented, with proposed solutions.

STRUCTURE COMPONENTS

The fabrication of the MAP structure requires high precision in critical dimensions. For example, the slot line-width has a tolerance of 10%, which allows 10-20nm variation from design. Thickness control on the films used (typically ~100nm) must achieve results within 5nm of design values. In addition, good uniformity in thin films and smooth interfaces between different materials are also important. To meet those requirements, electron beam lithography and lift off techniques were used to fabricate the nano-slots, and sputtering deposition was used to make the dielectric thin films. SEM images of those components are shown in Figure 2. Fig. 2(a) shows a test pattern of the nano-slots by electron beam lithography, with line width less than 100nm. Fig. 2(b) shows a cross-section SEM of the ZrO_2/HfO_2 Bragg reflector, where a 30kV ion beam is use to cut into the slab and the cross-section of the reflector is imaged with a 10kV electron beam. On the very top of the stack is a thin layer of gold which is deposited to avoid charging during electron imaging. Thin film measurements show that the film thicknesses are within ±5nm of design; this level of error (less than 5%) does not significantly change the resonant frequency or field profile of the structure.
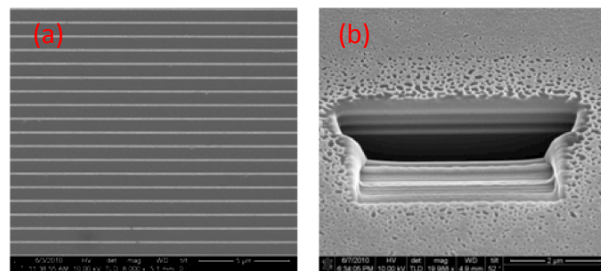

Figure 2: SEM image of the test coupling slots structure patterned by electron beam lithography (a), and cross-section SEM of the Bragg reflector showing althernating layers of ZrO_2/SiO_2 with precision thickness control.

The refractive indices of the thin films are measured by ellipsometry, and the results are shown in Fig. 3. For all thin films, the refractive index decreases with wavelength. At 800nm, the indices for ZrO_2, HfO_2 and SiO_2 are 2.17, 1.88, and 1.45, respectively.
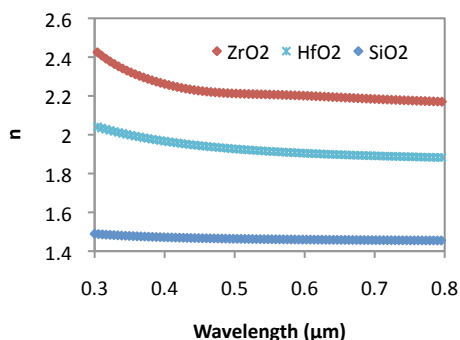

Figure 3: Refractive index profile of ZrO_2, HfO_2 and SiO_2 thin films measured from 300nm to 800nm.

As mentioned earlier, laser damage threshold is an important factor to consider for such a MAP strcuture. The damage threshold for a given laser and a given material depends mostly on the thin film packing density and the number of defects (such as impurities). Measurement of the laser damage threshold was carried out at SLAC using 800nm laser with 1.8ps pulses[6]. The beam size was about $8\times9\mu m^2$. In the experiment, a HeNe laser was co-incident with the 800nm laser on the sample. The criterion for damage was a change in the reflection of the HeNe probe after the sample was exposed to the IR pulses. The change in the HeNe reflection indicates that a change in the morphology of the surface, in other words damage, has occurred. For each sample, 192 measurements were taken. Fig. 4 shows the laser damage test results for the thin films we made. For ZrO_2 and SiO_2 single films, the laser damage thresholds are 3.97 J/cm^2 and 4.10J/cm^2, respectively. For a single pair ZrO_2/SiO_2 reflector, the damage threshold dropped down to about 2.5 J/cm^2. Note that these damage thresholds correspond to peak electric fields on the order of ~1GV/m. Given an enhancement factor of 10-15[1], the incident laser field of only ~100MV/m is required to achieve the projected accelerating field of 1GV/m. Therefore these materials are more than sufficient to meet the MAP requirements in terms of damage threshold.
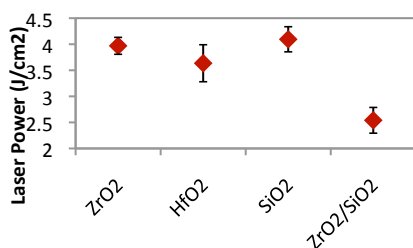

Figure 4: Laser damage threshold of dielectric thin film samples using 800nm, 1.8ps laser pulses. Bars indicate the range of results from 192 measurements.

FULL STRUCTURE

The MAP contains a periodic array of coupling slots at the drive laser wavelength, and ~1000 periods are required to achieve significant energy gain. Simulation results give optimal dimensions for the coupling slots of 286nm wide and 250μm long. Fig. 5 below shows the top view of a full scale slot structure made using HfO_2, with measured slot width 287.6nm, differing only by a negligible 1.6nm from the simulation design. The slots are free from overhanging structures on the side or top surface, although the edge does show some nanoscale roughness. Whether the rough edge can cause interface defects and make the structure prone to laser damage is uncertain at this point, and will be discovered later in laser damage testing of the full structure.
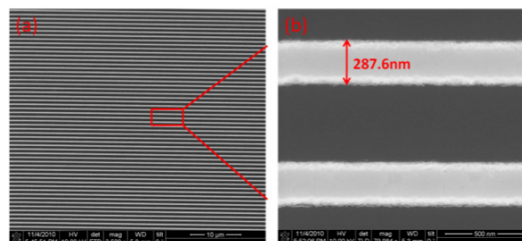

Figure 5: Top view SEM images of a full scale slotted structure with 1000 periods.

Following patterning of the slots, ZrO_2 was sputter deposited onto the sample to the thickness of about 300nm, and then planarized and polished to a final thickness of 90nm. Matching layers and Bragg reflector were subsequently fabricated on this planarized surface using sputter deposition. Cross-section SEM images of the structure are shown in Figure 6. Fig. 6(b) shows (from bottom to top) the ZrO_2 slots surrounded by HfO_2, 3 matching layers (SiO_2/HfO_2/SiO_2), and a ZrO_2/SiO_2 Bragg reflector. Note that the slots are not perfectly rectangular, but tapered on the bottom. Earlier simulation has shown that slight tapering in a single layer metal structure does not severely affect the resonance [7]. Here we assume the same and will verify that in the near future. One problem shown in Fig. 6(a) is that particles are trapped inside the films, resulting in many bubble structures on the surface. This is caused by residual slurry particles from the chemical mechanical polish process, and can be cleaned by mechanically scrubbing using a polyvinyl alcohol (PVA) sponge.
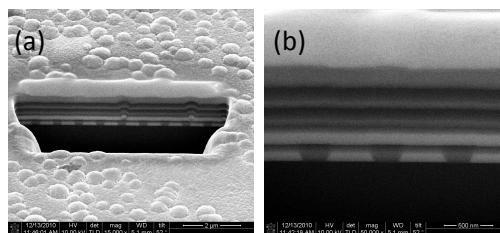

Figure 6: Cross section SEM image of the top slab structure, showing slight tapering in the slots (a) and particles trapped in between the thin films (b).

All the above described processes were transferred to fused silica substrate to fabricate an actual device for laser and electron beam test, with a few modifications. First, due to the nonconductive property of the substrate, a thin film of gold layer is deposited for electron beam lithography, and stripped at the end of the process. Second, due to the substrate's optical transparency at visible wavelengths, thin film thickness measurement is difficult, and this is especially challenging for the CMP process where optical measurement is used to measure and control the polish thickness. To overcome this, we run parallel processes on both Si and fused silica substrate, where the Si substrate serves the purpose of process optimization and device characterizations, and fused silica samples are used for bench tests.

STRUCTURE INTEGRATION

To run bench tests on the prototype structure, the top and the bottom slabs need to be integrated to form an 800nm vacuum gap in a precise and repeatable manner. One possible approach is to monolithically build up the whole structure on a single substrate. This approach has the advantage of precision and repeatability, but in practice it has two challenges. First, the slab structure above the vacuum gap, which is roughly 1μm thick, 250μm wide, and a few millimeters long, has support only on the peripheries. This thin membrane is likely to sag due to gravity and thus change the gap width, which will affect the resonance profile. Second, this vacuum gap is formed in the last step using a wet etch technique. The thin membrane above the vacuum gap is easily destroyed by the rinsing and drying process after the wet etch, as shown in Fig. 7.
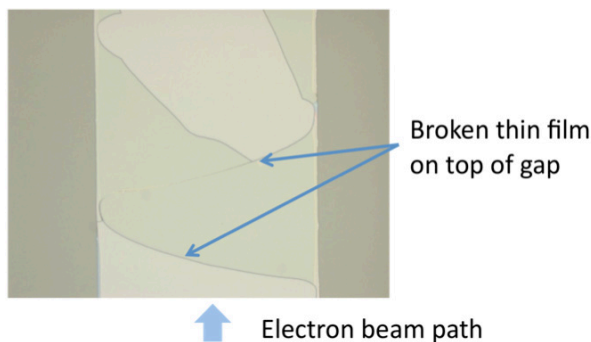

Figure 7: Optical image of a vacuum gap formed between 400nm SiO_2 thin film and Si substrate, where the thin film has been broken after the wet etch process

To avoid the sagging and rupture problem in the thin films, a second approach is proposed. In this approach both the bottom slab and the top lab are built separately on two substrates. A spacer that is 800nm thick is patterned on either slab, which leaves a 250μm wide channel for electron path. The two slabs can be bonded together using wafer bonding techniques, or simply clamped together for quick bench tests. This approach overcomes the problems associated with the monolithic

method, but in simulation, the substrate on the top seems to change the resonance profile. Further investigation of this effect, and/or further optimization of the resonance, is planned.

FUTURE WORK

In summary, a prototype micro accelerator structure has been successfully fabricated on Si substrate with optimized process parameters. A few modifications have been developed to apply this fabrication process to fused silica substrate, and a complete optical structure has been fabricated successfully on this new substrate and is ready for bench testing. However, since this whole structure is made from colorless, transparent dielectrics, it is difficult to identify the structure location on the chip optically, therefore is difficult to test the structure. A set of metal alignment marks can be patterned in close proximity to our test structure for quick and precise identification of the structure location. Future work will include laser damage test on the full slab structure, integration of the two slabs, resonance measurements with the drive laser, and finally electron beam injection and beam acceleration measurements.

ACKNOWLEDGEMENT

REFERENCES

[1] J. McNeur, J. B. Rosenzweig, G. Travish, J. Zhou, R. Yoder, 14th Advanced Acceleration Concepts Workshop, 2010 (AIP Conf. Proc. 1299) pp. 427-432.

[2] J. Zhou, J. McNeur, R. Yoder, G. Travish, J. B. Rosenzweig, 14th Advanced Accelerator Concepts Workshop, 2010,(AIP Conf. Proc. 1299) pp. 433-438.

[3] J. McNeur, J. B. Rosenzweig, G. Travish, J. Zhou, R. Yoder, presented at this conference.

[4] G. Travish, J. B. Rosenzweig, J. Xu, Proceedings of EPAC08, pp. 2827–2829.

[5] R. B. Yoder, G. Travish, J. Xu, J. B. Rosenzweig, 13th Advanced Acceleration Concepts Workshop, 2008 (AIP Conf. Proc. 1086), pp. 496–500.

[6] K. Soong, E. Colby, C. McGuinness, presented at this conference.

[7] R. B. Yoder, G. Travish, J. Xu, J. B. Rosenzweig, 13th Advanced Acceleration Concepts Workshop, 2008 (AIP Conf. Proc. 1086), pp. 496-500.